Nucleation Quality and Bubble Momentum and Their Effect on Droplet Velocity and Stability

Robert Cornell
Lexmark International Inc.
Lexington, Kentucky

Abstract

A recent paper, presented at NIP12 in San Antonio, described the relationship between heater power density and bubble nucleation. While the experimental results validated the model, it left an unanswered question, that is; what is the effect of power density and bubble nucleation on jetting performance? Increasing firing frequencies combined with more dense heater arrays act together to decrease the time available for pulsing individual heaters. This pushes power density upwards. However, thin film reliability issues often work in the opposite direction. Lower power density pulses, in general, permit longer heater lifetimes. Independent of these issues, there are jetting performance considerations. While heater lifetime effects are important, only the jetting performance issues are examined in this paper. In particular, this paper deals with droplet velocity and stability and their relationship to heater power density. Experimental data is presented along with simulation results. Bubble momentum is computed and used to explain the nonlinear velocity response to heater power density. Also, the spread of nucleation probability across the heater surface, is used to compute nucleation quality. The nucleation quality term has a direct relationship to the power density regime responsible for bubble instability induced droplet velocity variation.

Introduction

Thin film resistors are the fundamental building blocks of a thermal ink jet device. Thin film resistors are simple to understand and design, from an electrical viewpoint. In a thermal ink jet device, the total area consumed by these passive electrical components is a mere 0.5% of the silicon real estate. However, because they are the interface between the electrical domain and the heat transfer - fluid dynamics - phase change domain, the overall function of thermal ink jet resistors is anything but passive and simple. The complexity of simulating the interaction between these domains cannot be overstated, as evidenced by the following quote from a recently published CFD text [1].

> *"In applications involving multiphase flows, boiling, or condensation, especially in complex geometries, the experimental method remains the primary source of design information. Progress is being made in computational models for these flows but the work remains in a relatively primitive state compared to the status of predictive methods for laminar single phase flows over aerodynamic bodies."*

Primitive though it may be, the application specific model developed at Lexmark has evolved over the past several years into a predictive design tool. Also, it provides some insight into the physics of thermal ink jet processes that are too difficult to measure, and simulation remains the only viable technique.

Bubble Nucleation

When current passes through the thin film resistors of a thermal ink jet device, Joule heating on the order of 10^8 K/s results. Heating rates of this magnitude create homogeneous nucleation of ink at the resistor surface. Because homogeneous nucleation occurs at the ink's superheat limit, it is a predictable and repeatable phenomenon, removing the vagaries of surface condition induced heterogeneous nucleation. However, the exact superheat limit of ink has been the subject of some debate in the ink jet literature. It is common to find references to nucleation temperatures as low as 27°C [2] and some empirical models that predict temperatures exceeding the critical point under certain heat flux conditions [3][4]. Because nucleation temperature determines the magnitude of the pressure pulse, and the pressure pulse is the driving mechanism for fluid flow, no useful bubble dynamics simulation can proceed with such an uncertain starting point.

In response to the ambiguity in the literature, a recent paper discussed the various nucleation models and went on to derive a nucleation probability function [5] based on kinetic theory, unsteady heat transfer and reliability statistics. Figure 1 shows a typical output from the bubble reliability model. This plot is a snapshot of nucleation probability across the heater surface during a high power density fire pulse. Figure 2 is similar, except it shows nucleation probability during a low power density fire pulse. There will be more discussion of the significance of these later. Figure 3 shows the correlation between simulated bubble reliability results and a set of experimental data. The empirical data in this plot spans three heater designs, open and closed pool testing, DI water and dye based ink. Statistical analysis indicates the bubble reliability model can explain 96% of the variability in the lab data. Clearly, the bubble reliability model is a reasonable predictor of nucleation probability. However, it is unclear from Figure 3 whether there is any advantage, or disadvantage, of pulsing the heaters with any particular power density.

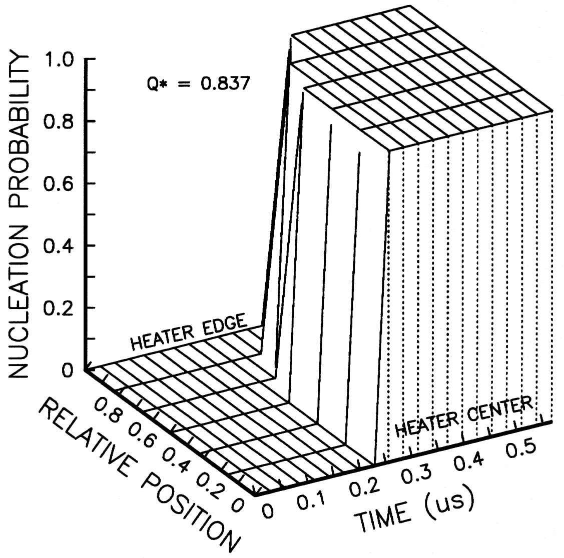

Figure 1. Bubble Reliability - High Power Density Pulse

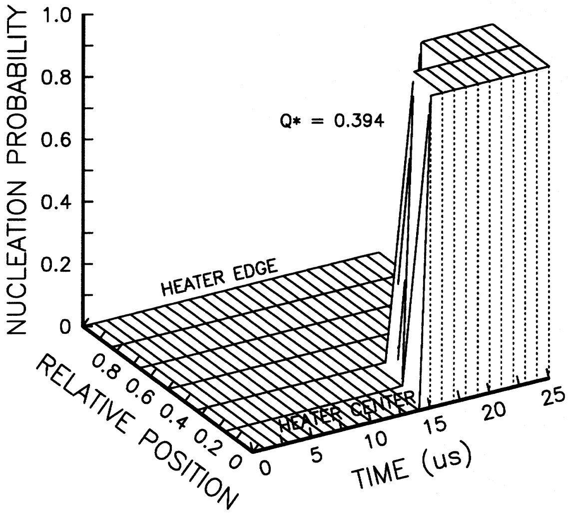

Figure 2. Bubble Reliability - Low Power Density Pulse

Droplet velocity measurements as well as print quality comparisons indicate that power density does indeed matter. Figure 4 is a compilation of velocity data across three widely varying print head designs. This data was taken with extremely long cycle times to guarantee there were no meniscus oscillations, or nozzle plate flooding effects to confound the experiment. Several observations can be made. The low power density region, to the left of the maxima, has sharply decreasing droplet velocity and wildly increasing velocity variation. The high power density region, to the right of the maxima, shows a slight decrease in droplet velocity, yet no velocity variation. The Bubble Dynamics - Phase Change Model will be used to explain this data set.

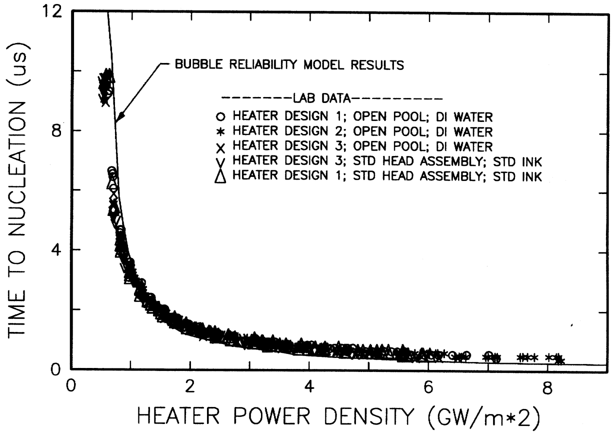

Figure 3. Lab Data and Bubble Reliability Simulation Results

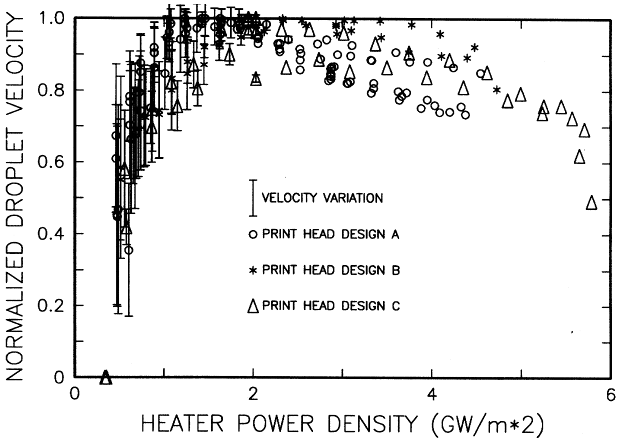

Figure 4. Droplet Velocity and Stability Data

Power Density and Velocity Stability

The electrical connection to the heater is made with aluminum. Aluminum is a popular thin film wiring metal because it's an excellent conductor of current. However, it's also an excellent conductor of thermal energy. This means the heater edge, at the aluminum interface, will be much cooler than the heater center due to thermal diffusion during the fire pulse. Two dimensional heat transfer simulations, as well as heater oxidation patterns, show this clearly. Because the heater surface is not isothermal, ink does not reach the superheat limit over the entire heater at the same instant. This is evident from the bubble reliability simulations of Figures 1 and 2. The nucleation process is spread over a much longer time in the low power density case. It will be shown that spreading out nucleation probability over a longer time period negatively affects droplet velocity stability.

Ideally, the entire heater surface has a bubble reliability of unity at the same instant, but as explained above this is not possible due to the cooling effect of aluminum electrodes attached to the heater. Once nucleation begins at the heater center there is a race between the advancing bubble wall and nucleation probability in other regions of the heater. To enjoy homogeneous nucleation across the heater surface, the bubble wall must lose this race. Low power density fire pulses generate low heat flux and slowly propagating temperature fields. Slowly propagating temperature fields create a situation where the hot bubble wall must grow into a cooler region before the fire pulse has ended. If it takes a long time to reach temperatures sufficient for nucleation in regions away from the heater center, the advancing bubble wall will quickly grow into a portion of the heater too cold to sustain growth, so it will begin to collapse. But later in the fire pulse this region may reach the superheat limit. This process causes an alternating expand/collapse activity at the bubble wall.

Open pool bubble watching has confirmed that vapor bubbles created by low power density pulses are ragged and erratic, consistent with an alternating expand/collapse activity at the bubble wall. Conversely, it has been observed that bubbles created by high power density fire pulses are smooth and repeatable. Since the data shown in Figure 4 was taken at cycle times about 400X greater than the refill times, meniscus dynamics cannot explain the droplet velocity variation. However, it is a likely hypothesis that ragged, unstable bubble dynamics are responsible for droplet velocity variation in the low power density region, and smooth, repeatable bubbles are credited with the stable droplet ejection that's characteristic of the high power density region. To mathematically describe the velocity stability - power density relationship, it is necessary to introduce a new term called nucleation quality.

Nucleation Quality

To compute nucleation quality, it is first necessary to compute bubble reliability. Space doesn't permit showing the details here, but it is fully described in Reference [5]. Suffice it to say, bubble reliability is a function of the unsteady temperature field and the molecular kinetics of ink. Since ink is about 90% water, on a mole basis, all calculations assume the molecular kinetics of ink can be modeled as water. The correlation shown in Figure 3 indicates that this is a reasonable assumption.

R = bubble reliability = nucleation probability (Ref. 5)
L^* = heater region where ($R = 1$)
L_N = heater region where ($R < 1$)
$L_H = L^* + L_N$ = total heater length
Q^* = nucleation quality
Q_N = not quality
β = heater activation rate
S = nucleation spread factor
t = time

$$Q^* = L^* / L_H \tag{1}$$

$$Q_N = L_N / L_H = 1 - Q^* \tag{2}$$

Writing (2) as a rate equation:

$$dQ_N / dt = (1 / L_H)\, dL_N / dt \tag{3}$$

Tracking the spread of nucleation probability during the fire pulse allows heater activation rate (β) to be computed:

$$\beta(t) = [-1 / L_N]\, dL_N / dt \tag{4}$$

Substitute (3) into (4):

$$\beta(t) = (-1 / Q_N) dQ_N / dt \tag{5}$$

Integrating (5) over the fire pulse with the initial conditions defined by: $L_N(0) = L_H$; $Q_N(0) = 1$

$$Q_N = \exp(-S) \tag{6}$$

$$S = \beta(t) \text{ integrated over the fire pulse} \tag{7}$$

Then by equation (2):

$$Q^* = 1 - \exp(-S) \tag{8}$$

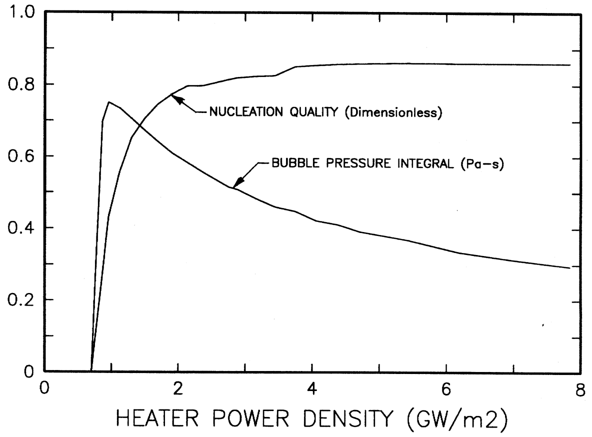

Figure 5. Nucleation Quality and Bubble Pressure Integral

Using the method described above, nucleation quality was computed for a wide range of power densities. The results are shown in Figure 5. It is evident that nucleation quality drops off sharply in the low power density region, and it is flat in the high power density region. This is consistent with the velocity variation characteristics shown earlier in Figure 4.

Power Density and Velocity

While stability may be optimum in the high power density region, there is an overall decline in droplet velocity. As power density increases, the heating rate of the thin film structure increases. As stated earlier, homogeneous nucleation begins when ink at the heater surface reaches the superheat limit. It is obvious from Figure 3 that low power density conditions will require very long fire pulses. Conversely, high power density pulses cause the nucleation event to occur quickly, limiting heat transfer into the ink. While it is true that high power density conditions mean higher heat flux into the ink, it is also true that the heat flux relation in Figure 3 is linear with heater power density, but the time to nucleation decreases exponentially. This exponential decrease in time to nucleation limits the thermal energy available for fueling the phase change process. It will be shown that this is the primary cause of the velocity decrease in the high power density region.

Bubble Pressure and Phase Change

Since homogeneous nucleation creates a vapor explosion, and this vapor explosion is ultimately responsible for fluid motion and droplet ejection, it is first necessary to compute the magnitude of this impulse. A convenient measure of this is the bubble pressure integral, i.e. the area under the pressure-time curve. Incidentally, the fact that homogeneous nucleation results in a vapor explosion has recently been denigrated. Yet the evidence proves otherwise for ink jet applications. First of all, the temperature gradients are so steep, the thermal boundary layer is just a micron or two thick, and only ~300 ppm of the water molecules in the bubble chamber undergo a reversible phase change. Indeed, boiling at the superheat limit produces an extremely large pressure, but this is not a disadvantage. Quite the contrary, it is this high pressure pulse that provides thermal ink jet one of it's advantages over competing technologies. Generating an instantaneous pressure of 100+ atmospheres at nucleation gives thermal ink jet a powerful advantage for clearing viscous nozzle plugs and air bubbles that are endemic of all water based ink jet technologies.

To describe the power density - droplet velocity relationship with the bubble pressure integral, it is first required to compute the phase change physics. If the bubble pressure - time history is known, a numerical solution to the flow field may be obtained with a general purpose commercial CFD package. However, the liquid - vapor phase change renders bubble pressure a dependent variable, not a model input. While most general purpose CFD packages claim to handle multiphase flow, they do not compute the actual phase change physics. Since this is the driving mechanism behind fluid flow in a thermal ink jet device, a short discussion of this limitation is warranted.

While the genesis of thermal ink jet fluid flow is a high pressure impulse, the flow itself is well behaved - inside the bubble chamber and nozzle it is laminar and incompressible. Since the flow is incompressible, the mathematical behavior of the pressure field is elliptic. A well posed elliptic pressure field problem must have pressure at the boundaries completely defined. But the pressure at the moving bubble wall is unknown due to the phase change, making this a Stefan moving boundary problem. This an important distinction. While the mixed Dirichlet - Neumann boundaries are readily handled, it is impossible to obtain an analytical solution for a two dimensional Stefan moving boundary problem [6]. Numerical solutions must be obtained. The unknown pressure boundary due to the liquid-vapor phase change combined with the steep temperature gradient at the bubble wall causes even the numerical methods to deviate from typical incompressible flow algorithms.

Because of the liquid-vapor phase change at the moving bubble wall, the complete set of conservation equations must be solved simultaneously, whereas a typical incompressible flow-heat transfer problem can decouple the solution of the temperature field from the pressure and velocity fields [7]. This distinction makes the solution vector look more like a compressible flow problem, but solution algorithms used in compressible flows are not suitable for the thermal ink jet problem. Let's first consider the computational cell size. Because the temperature gradient at the bubble wall is on the order of 10^8 K/m, the grid size in the vicinity of the bubble wall must be about 1 nanometer in length. This cell size limits the time step to about 10^{-22} seconds to satisfy the momentum diffusion stability condition. The combination of the Stefan boundary condition, elliptic behavior pressure field and steep temperature gradients make it impractical to use a compressible flow algorithm to simulate the phase change process in a thermal ink jet device.

Although it presently lacks the sophisticated free surface construction algorithms typical of commercial CFD packages, the Bubble Dynamics - Phase Change model does solve the conservation equations and account for heat transfer - phase change at the moving bubble wall. Details of the model cannot be described here due to space limitations. Suffice it to say, one of the model outputs is the bubble pressure - time history. This output is used to compute the flow field and the bubble pressure integral. The bubble pressure integral explains the declining droplet velocity that's characteristic of the high power density region.

Bubble Pressure Integral

A typical bubble impulse is shown in Figure 6 for a low power density driving condition. The area under the curve represents the bubble pressure integral. Contrasting this is the pressure history, also shown in Figure 6, for a high power density driving condition. Even though both cases have the same initial pressure, note the significant difference in the bubble pressure integral for these two power density conditions. Because the high power density case reaches nucleation temperatures quickly, it does not have the time to transfer much thermal energy into the ink. As described earlier, this means less energy is available for phase change. This causes the bubble wall to cool more rapidly, as evidenced by the shorter time required for bubble pressure to reach atmospheric in the high power density case.

$$I = \text{Integral of } P(t) \text{ from } t^* \text{ to } t_1 \qquad (9)$$

I = bubble pressure integral (Pa - s)
$P = P_V - P_0$ (Pa)
P_V = bubble vapor pressure (Pa)
P_0 = atmospheric pressure (Pa)
t^* = onset of nucleation (s) i.e. when $Q^* \rightarrow 1$
t_1 = the time during which ($P > P_0$)

The Bubble Dynamics-Phase Change model was used to compute the bubble pressure integral as a function of heater power density. Heater energy density was held at 4300 Joules/m^2 for these calculations. The results are shown in Figure 5. The reason this curve decreases on the right hand side is due to the heat transfer limiting, rapid nucleation times with high power density pulses. The sharp drop on the left hand side of the curve is due to the long fire pulses allowing lateral diffusion the time to rob thermal energy to the point where none of the heater surface reaches the ink superheat limit.

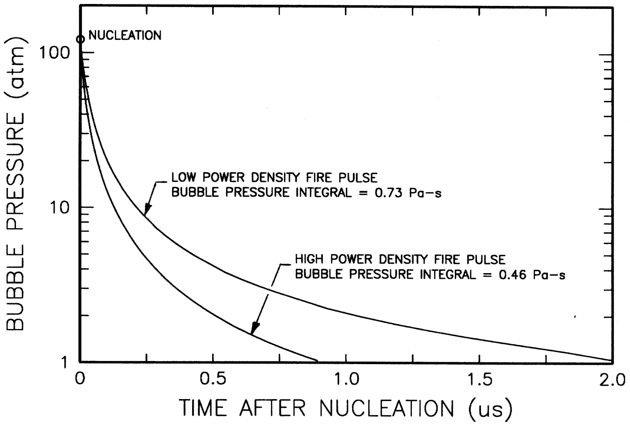

Figure 6. Bubble Pressure Versus Time

Bubble Momentum

The bubble pressure integral has units of Pascal-seconds. Multiplying this by heater area produces a term with units of Newton-seconds, in other words a momentum term. Since the job of the bubble is to impart momentum to the surrounding ink, it is a logical expectation that bubble momentum and droplet momentum are somehow linked. However, the entire heater does not participate in the nucleation process, as described earlier. Given this argument, it may be reasonable to assume the following product will be descriptive of the relationship between heater power density and droplet momentum:

$$M_B = (I)(A_{htr})(Q^*) \quad (10)$$

M_B = *Bubble Momentum (N-s) or (kg m/s)*
I = *Bubble Pressure Integral (Pa -s)*
$Ahtr$ = *Heater Area (m^2)*
Q^* = *Nucleation Quality*

Each of the data points from Figure 4 had an associated droplet mass data point as well. Since the product of mass and velocity is also a momentum term, it would be interesting to compare the droplet momentum and bubble momentum response curves. This is shown in Figure 7. It is evident, the computed bubble momentum curve accurately reflects the droplet momentum response to heater power density.

Product Similarities

Interestingly, the data in Figure 7 was from several widely varying print head designs, yet the response characteristics could all be described by a single, normalized bubble momentum curve. In a similar vein, all of the data from Figure 3 could also be described by a single bubble reliability curve. Why should all these print heads have a similar response to heater power density? The answer to this question focuses on similarities between the transient temperature fields when power and energy are considered on a unit heater area basis. The nonlinear characteristics of the experimental data were all accounted for by thermal effects. While heater size and shape differed, the vertical thin film structure was the same across all these designs. Then it stands to reason, the thermal response of these designs was the same on a power per unit heater area basis. Further evidence of this fact is illustrated in Figure 8, where three different heater designs show the same response to energy per unit heater area.

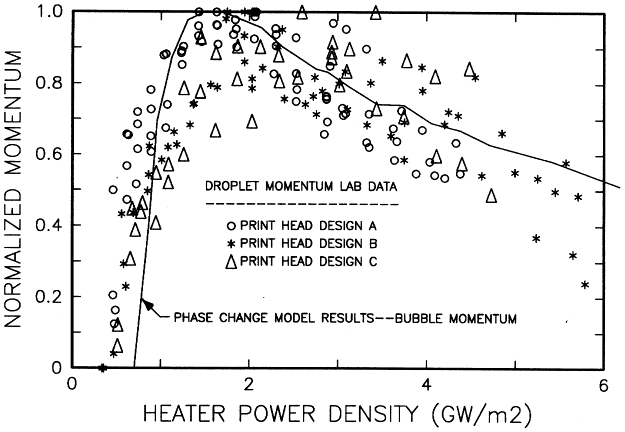

Figure 7. Momentum Lab Data and Simulation Results

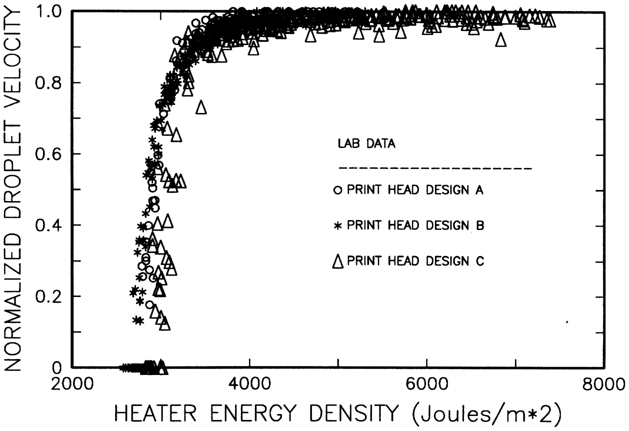

Figure 8. Velocity Versus Energy Density Lab Data

Conclusion

When cycle times are large enough to negate meniscus dynamic effects, the velocity - heater power density response curve has several characteristics that are similar across widely varying print head designs. The low power density region is characterized by low velocity, unstable jets. The high power density region is characterized by stable jets that show a slight velocity decrease. Using the Bubble Dynamics - Phase Change simulation package, the underlying mechanisms have been explained. Velocity instability is the result of alternating expand/collapse bubble dynamics due to slowly propagating temperature fields and low quality bubble nucleation. The declining velocities in both the high power density and low power density regions can be explained with the bubble momentum term. The bubble momentum - power density response curve has strikingly similar characteristics to measured droplet momentum data across a wide range of print head designs.

References

1. J. Tannehill, et.al., *Computational Fluid Mechanics and Heat Transfer*, 2nd ed., Taylor & Francis, Washington, DC., p5, 1997.
2. A. Mirfakhraee, “An Analysis of the Growth and Collapse of Vapor Bubbles in Ink-Jet Printers”, *IBM Research Report RJ6823*, (1989).
3. W. Runge, “Nucleation in Thermal Ink-Jet Printers”, *IS&T 8th Intl. Cong. Adv. in Non-Impact Printing Tech.*, (1992).
4. J. Poppel, “Indirect Measurement of the Nucleation Temperature at the Heater of a Bubble Jet”, *Proc. IEEE*, (1989).
5. R. Cornell, “A Theoretical and Experimental Examination of Thermal Ink Jet Nucleation Criteria”, *IS&T NIP12 Intl. Conf. Digital Printing Tech.*, (1996).
6. G. Segal, et.al., “A Conserving Discretization for the Free Boundary in a Two Dimensional Stefan Problem”, *J. Comp. Physics*, **141**, (1998).
7. J. Anderson, Computational Fluid Dynamics, McGraw Hill, NY, 1995.

Biography

Robert Cornell is a Senior Engineer in the Lexmark Ink Jet Technology Department. His main research interests include heat transfer and bubble dynamics from experimental and CFD viewpoints. He received his formal training as a Mechanical Engineer at the University of Pittsburgh. He is also an ASQC Certified Reliability Engineer. Since 1977 he has been involved in a wide range of printer development programs at IBM and Lexmark.